C. R. Physique 3 (2002) 153–161

Physique statistique, thermodynamique/*Statistical physics, thermodynamics*
(Solides, fluides : propriétés mécaniques et thermiques/*Solids, fluids: mechanical and thermal properties*)

DOSSIER

PHYSIQUE DE LA MATIÈRE EN GRAINS
PHYSICS OF GRANULAR MEDIA

Structures and non-equilibrium dynamics in granular media

Stefan Luding [a,b]

[a] **Institute for Computer Applications 1, University of Stuttgart, Pfaffenwaldring 27, 70569 Stuttgart, Germany**
[b] **DelftChemTech, TU Delft, Julianalaan 136, 2628 BL Delft, The Netherlands**

Received 14 September 2001; accepted 11 December 2001

Note presented by Guy Laval.

Abstract In granular media, dissipation leads to interesting phenomena like cluster formation in non-equilibrium dynamical states. As an example, the freely cooling system is examined concerning the energy decay and the cluster evolution with time. Furthermore, the probability distribution of the collision frequency is discussed. Uncorrelated events lead to a Poisson distribution for the collision frequencies in the homogeneous system, whereas cooperative phenomena can be related to a power-law decay of the collision probability per unit time. ***To cite this article: S. Luding, C. R. Physique 3 (2002) 153–161.*** © 2002 Académie des sciences/Éditions scientifiques et médicales Elsevier SAS

inhomogeneous free cooling / clustering / cooperative phenomena / event-driven molecular dynamics

Résumé Dans les milieux granulaires, la dissipation conduit à des phénomènes intéressants comme la formation d'amas dans des états dynamiques hors-équilibre. A titre d'exemple, nous examinons la perte d'énergie et l'évolution des amas avec le temps d'un système qui se refroidit librement. De plus, nous analysons la distribution de probabilité de la fréquence de collision. Dans un système homogène, la fréquence de collision d'événements non corrélés conduit à une distribution de Poisson, alors que les phénomènes coopératifs sont caractérisés par une probabilité de collision par unité de temps qui décroît comme une loi de puissance. ***Pour citer cet article : S. Luding, C. R. Physique 3 (2002) 153–161.*** © 2002 Académie des sciences/Éditions scientifiques et médicales Elsevier SAS

refroidissement libre et inhomogène / phénomènes coopératifs / dynamique moléculaire gérée par les événements

1. Introduction

Astonishing phenomena occur when granular material is studied [1–4]. The subject of this study is the pattern formation in a dissipative, freely cooling system [5–8]. The interesting behavior of granular media is connected to its ability to form a hybrid state between a fluid and a solid: energy input can lead to a reduction of density so that the material can flow, i.e. it becomes 'fluid'. On the other hand, in the absence

E-mail address: lui@ica1.uni-stuttgart.de (S. Luding).

S1631-0705(02)01308-7/FLA

of energy input, granular materials 'solidify' due to dissipation. This makes granular media an interesting multi-particle system with a rich phenomenology; however, theoretical approaches are non-classical and appear often extremely difficult, so that there is still active research directed towards the understanding of granular media.

The basic ingredients of a granular model material are discussed briefly in Section 2. The inhomogeneous cooling and clustering are described in detail in Section 3. The basic idea is that in a freely cooling granular gas, fluctuations in density and temperature cause a position dependent energy loss. Due to strong local dissipation, pressure and energy drop rapidly and material moves from 'hot' to 'cold' regions, leading to even stronger dissipation and thus causing the density instability with ever growing clusters. The probability distribution function for the collision frequency is measured in both the homogeneously cooling and the inhomogeneous clustering regime, where differences in the functional behavior are displayed [9]. The same phenomenon is also found in the flow through a pipe [10], where shock waves and arching are the observed cooperative phenomena.

2. Models for multi-particle simulations

The constituents of granular media are mesoscopic particles. When those objects interact (collide) the attractive potentials of the individual grains can be neglected. Two models for the repulsive particle–particle interactions are discussed in the following. They account for the excluded volume of the particles via a repulsive potential, either 'hard' or 'soft' and also account for dissipation in collisions via some coefficient of restitution. The third ingredient of a model granular material is friction which couples the rotational degrees of freedom to the linear motion, but it is not discussed in this paper.

The difference between the two most frequently used discrete element methods is the repulsive interaction potential. For the molecular dynamics (MD) method, soft particles with a power-law interaction potential are assumed, whereas for the event-driven (ED) method perfectly rigid particles are used. The consequence is that the duration of the contact of two particles, t_c, is finite for MD, but vanishes for ED.

2.1. The event-driven, rigid particle method

Consider two particles with diameter d_1 and d_2 and masses m_1 and m_2. The normal unit vector for their contact is n, and r_i is the vector to the position of the center of particle i ($i = 1, 2$). The relative velocity of the contact points is $v_c = v_1 - v_2$, with the velocity v_i of particle i. From momentum conservation it follows

$$v_1' = v_1 + \Delta P/m_1 \quad \text{and} \quad v_2' = v_2 - \Delta P/m_2, \tag{1}$$

where v_i' is the unknown velocity of particle i after collision. The change of linear momentum of particle 1 is a function of the coefficient of restitution r:

$$\Delta P = -m_{12}(1+r)v_c^{(n)}, \tag{2}$$

with the reduced mass $m_{12} = m_1 m_2/(m_1 + m_2)$ and the normal velocity $v_c^{(n)}$.

For the simulation of rigid particles, an event-driven method is used [7,11,12]. The particles undergo an undisturbed motion until an event occurs. An event can be either the collision of two particles or the collision of a particle with a wall. From the velocities just before contact, the particle velocities after a contact are computed following Eq. (1). Lubachevsky [11] introduced an efficient scalar ED algorithm which updates only those particles involved in the previous collision. The original algorithm is implemented and generalized to take into account dissipation.

2.2. The time driven, soft particle technique

Even without using the soft particle method [13–15] in this study, it is convenient to discuss briefly the standard approach. Replacing ΔP in Eq. (1) by $f(t)\Delta t_{\mathrm{MD}}$, with the molecular dynamics time step Δt_{MD}, allows the integration of the corresponding, discretized equations of motion with standard numerical methods [14].

Since the modeling of realistic deformations of the particles would be much too complicated, let us assume that the overlap of two particles is the only quantity important for the interaction potential. The interaction of two particles can be split into (at least) three independent forces, and is typically short range, i.e. the particles interact only when they are in contact. The first force, an elastic repulsive force proportional to the overlap, accounts for the excluded volume which each particle occupies. In the simplest case, a linear spring can be used. The second force, a viscous damping force, models the dissipation in the normal direction and is proportional to the relative velocity. The simplest possible dashpot is again linear. This linear spring-dashpot model can be solved analytically and leads to a constant contact duration t_{c} and a constant restitution coefficient r [16]. The third force, accounting for friction, acts in the tangential direction, but will not be discussed here; for more information, see [1].

2.3. The connection between hard- and soft-sphere models

In the ED method, the time during which two particles are in contact is implicitly zero. The consequence is that exclusively pair contacts occur and the instantaneous momentum change ΔP in Eq. (1) suffices to describe the collision. However, ED algorithms with constant r run into difficulties when the time between events, t_n, becomes too small—typically in systems with strong dissipation—and the so-called 'inelastic collapse' occurs [6,17], i.e. the collision rate diverges for a few particles in the system. Since this is an artefact of the hard sphere model, it is unphysical and has to be avoided. Because a diverging number of collisions is only possible if the contact duration vanishes, the physical contact duration t_{c} has to be reintroduced in order to allow for realistic ED simulations. In MD simulations, on the other hand, one has $t_{\mathrm{c}} > 0$, since every contact takes some finite time. Therefore, only a limited amount of kinetic energy ($\Delta E \propto 1 - r^2$) can be dissipated per collision. A finite contact duration implies a finite energy dissipation rate. In contrast, the consequence of a diverging collision rate would be a diverging energy dissipation rate.

In a dense system of real particles, energy dissipation becomes ineffective, i.e. the 'detachment effect' occurs [18,19]. This effect is not obtained with hard particles and a constant coefficient of restitution r. Therefore, in the framework of the so-called TC model, the restitution becomes elastic in nature, $r_{\mathrm{n}}^{(i)} = 1$, if collisions occur too frequently, i.e. $t_{\mathrm{n}}^{(i)} \leqslant t_{\mathrm{c}}$, for the collision n of particle i. The time since the last collision is $t_{\mathrm{n}}^{(i)}$ and the cut-off parameter t_{c} for elastic contacts can be identified with the contact duration. Thus, an additional material parameter is defined for the hard sphere model, that leads to qualitative agreement between ED and MD simulations and, in addition, avoids the inelastic collapse artefact. Recently, it has been shown that the TC model does not affect physical observables of the system, like the energy, as long as it is reasonably small [17].

3. Freely cooling granular media

The simulations presented in the following involve $N = 99856 = 316^2$ dissipative particles with the restitution coefficients $r = 0.9$, 0.8, and 0.6, in a periodic, quadratic system with volume fraction $\nu = 0.25$. The system size is $l = Ld$ with dimensionless size $L = 560$ and particle diameter $d = 1$ mm. In order to reach an equilibrated initial condition, the system is first allowed to equilibrate with $r = 1$ for several hundreds of collisions per particle, so that a Maxwellian velocity distribution and a homogeneous density can be found. Then, at $t = 0$ s, dissipation is activated and the quantities of interest are examined. Snapshots of the simulation with $r = 0.9$ are presented in Fig. 1 at different, rescaled times τ (see below).

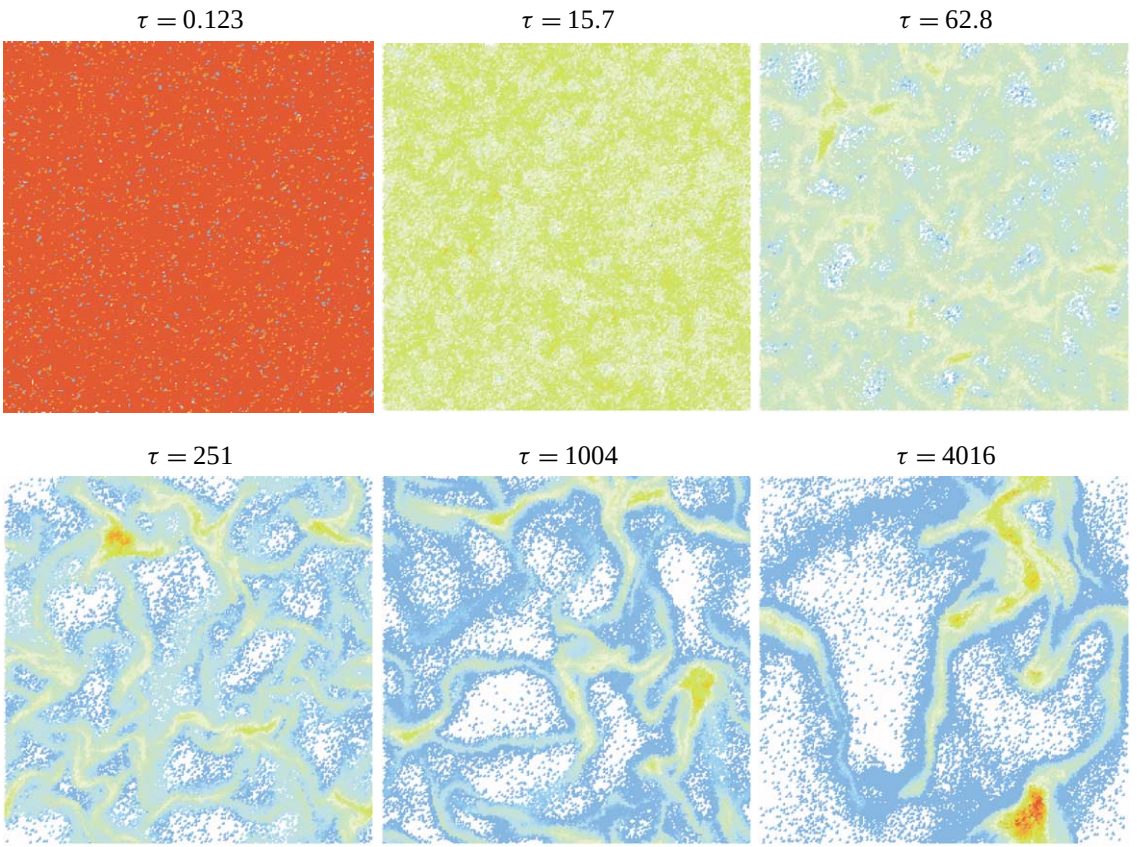

Figure 1. ED simulation with $N = 99856$ particles in a system of size $L = 560$, volume fraction $\nu = 0.25$, restitution coefficient $r = 0.9$, and critical collision frequency $t_c^{-1} = 10^5\ \mathrm{s}^{-1}$. The collision frequency is color-coded: red, green–yellow and blue correspond to collision rates $t_n^{-1} \approx 250\ \mathrm{s}^{-1}$, $50\ \mathrm{s}^{-1}$ and $10\ \mathrm{s}^{-1}$, respectively.

The first picture in Fig. 1 is taken in the initially homogeneous cooling regime, whereas the next four pictures show the different stages of the cluster growth regime. The final picture is taken in the limiting state, where the cluster has reached the system size. The particles are colored spots, where the green–yellow/red areas in the cluster centers correspond to particles with collision rate $t_n^{-1} \geqslant 50\ \mathrm{s}^{-1}$. This is much smaller than the critical collision rate $t_c^{-1} = 10^5\ \mathrm{s}^{-1}$, so that only a very small number of particles will be affected by the TC model.

3.1. Homogeneous and inhomogeneous cooling

In the homogeneous cooling state [6,20,21], one can expect that the kinetic energy $E = K(t)/K(0)$ of the system decays with time (the decay of energy with time is also evidenced by the change of color from red over orange to green and blue in Fig. 1) and follows the master-curve

$$E(\tau) = \frac{1}{(1+\tau)^2}, \tag{3}$$

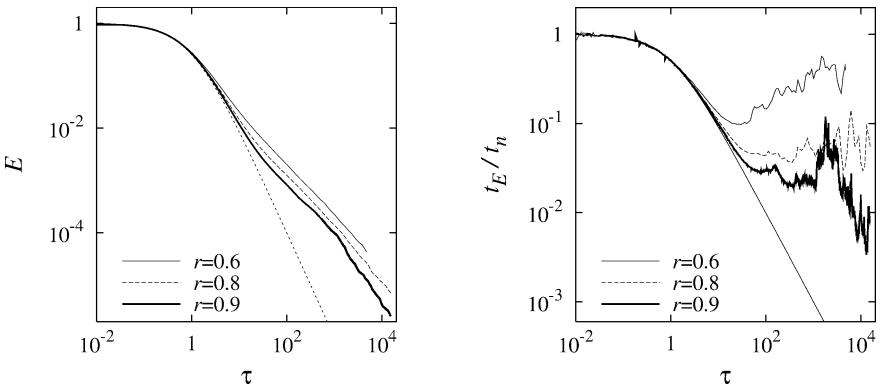

Figure 2. Left: kinetic energy E plotted against τ for different values of $r = 0.9$, 0.8, and 0.6. The dotted line represents equation (3). Right: normalized collision rate t_E/t_n plotted against τ. The solid straight line represents the collision rate $\sqrt{E}$ in the homogenously cooling case.

with the dimensionless time $\tau = (1-r^2)t/(4t_E)$, the collision rate $t_E^{-1} = 8\nu g(\nu)\bar{v}/(\sqrt{\pi}d)$, the mean velocity $\bar{v} = \sqrt{K(t)/Nm}$, and the increased contact probability $g(\nu) = (1 - 7\nu/16)/(1-\nu)^2$ due to excluded volume effects at finite volume fractions ν. Inserting the parameters from the simulation, $1-r^2 = 0.19$, $g(\nu) \approx 1.5833$, and $\bar{v} = 0.1444\,\mathrm{m/s}$, one obtains an initial collision rate $t_E^{-1}(0) = 258.05\,\mathrm{s}^{-1}$ (corresponding to the red color in Fig. 1).

In Fig. 2, the normalized kinetic energy E and the normalized collision rate $t_\mathrm{n}^{-1}/t_E^{-1}$, are presented, both as a function of the normalized time τ. At the beginning of the simulation we observe a perfect agreement between the theory for homogeneous cooling and the simulations. At $\tau \approx 10$–40 substantial deviations from the homogeneous cooling behavior become evident, i.e. the decay of energy is slowed down earlier for stronger dissipation. The deviation from the analytical form increases until $\tau \approx 10^3$ where the clusters reach system size and the behavior of E changes again to a slightly more rapid decrease.

This change in behavior is evident from the collision rate t_n^{-1}. At first, in the homogeneous cooling regime, the collision rate decays with $t_\mathrm{n}^{-1} \propto \sqrt{E}$. Then the collision rate is almost constant (for $r = 0.9$ and $r = 0.8$) or even increases (for $r = 0.6$), until at $\tau \approx 10^3$ it becomes very noisy, indicating another change in the collective behavior. The long-time power law for the decay of energy with time is -2 in the homogeneous cooling case. In the cluster growth regime, however, we obtain slopes slightly smaller than -1 (the best fit leads to -0.920, -0.927, and -0.941 for $r = 0.9$, 0.8, and 0.6, respectively, with errors ± 0.002).

3.2. Cluster structure

In Fig. 3, zooms into the bottom-right area of the system in Fig. 1 are presented. In the initial state, the system is rather disordered and homogeneous. In the cluster growth regime, some particles approach closer and form loose clusters, however, the structure is still disordered, fluid-like. Only in the very late stage of the simulation, where the clusters are very large, one obtains crystalline, triangular lattice structures with a peculiar distribution of collision rates as color-coded.

This more qualitative picture can also be verified by computing the particle correlation function $g(r/d)$, see Fig. 4. The data are displayed for different τ-values, showing that the structure in the system becomes more and more pronounced with increasing time. Like the zoom-in in Fig. 3, the correlation function also shows that the crystalline structure occurs only in the late regime where the clusters are very large, with 'frozen' cores. Pronounced peaks at 1, $\sqrt{3}$, 2, ... indicate a triangular order of the particles.

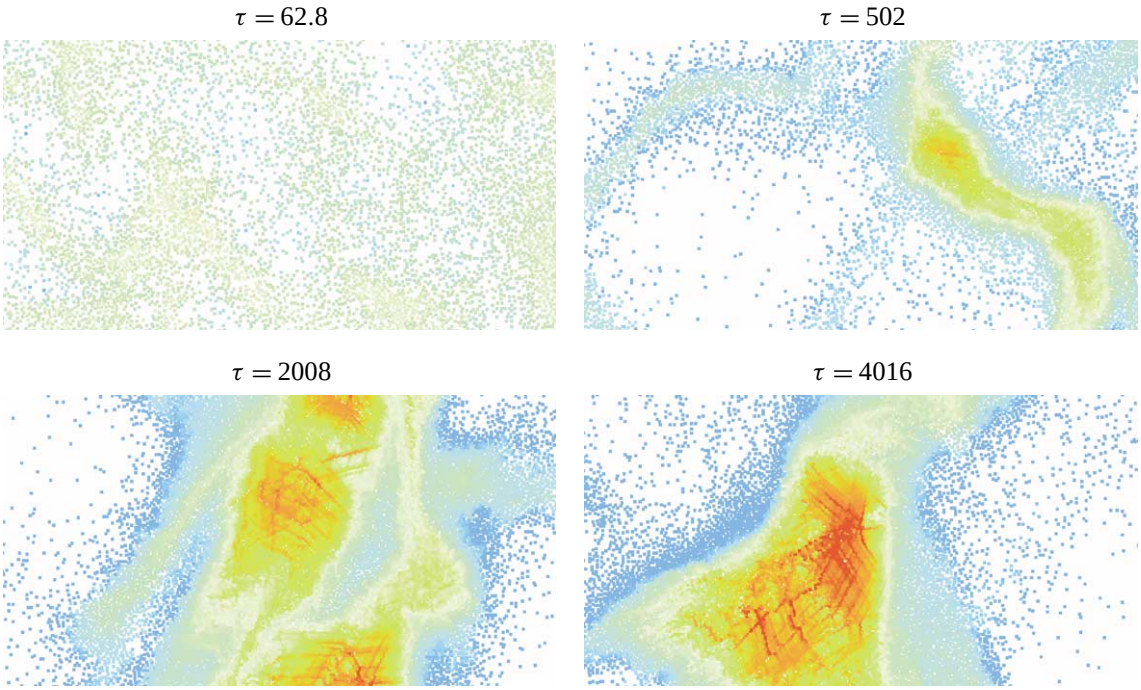

Figure 3. Zooms into the lower right part of the ED simulation from Fig. 1.

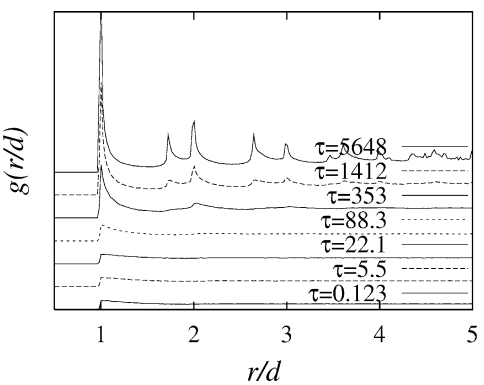

Figure 4. Correlation function $g(r/d)$ as obtained from the simulation in Fig. 1. The different curves are shifted vertically in order to avoid overlap and τ is given in the inset.

3.3. Cluster growth

The cluster growth can be studied quantitatively in the spirit of Luding and Herrmann [7]. All particle pairs with a distance smaller than some cut-off distance $\delta < (1 + S)d$, with an arbitrary cut-off parameter $S = 0.1$, are assumed to belong to the same cluster. After all particle pairs are examined, one obtains a cluster-size distribution and its moments. The first moment, the mean cluster size $\langle M \rangle$, and the size of the largest cluster $M_{\max}$ are plotted in Fig. 5 against the time τ.

Both values are almost constant in the initial, homogeneous cooling regime. In the cluster growth regime a rapid increase of both $\langle M \rangle$ and $M_{\max}$ is evidenced until, at larger τ, the values reach a maximum and seemingly saturate or even decrease in the final regime where the clusters have reached system size. The

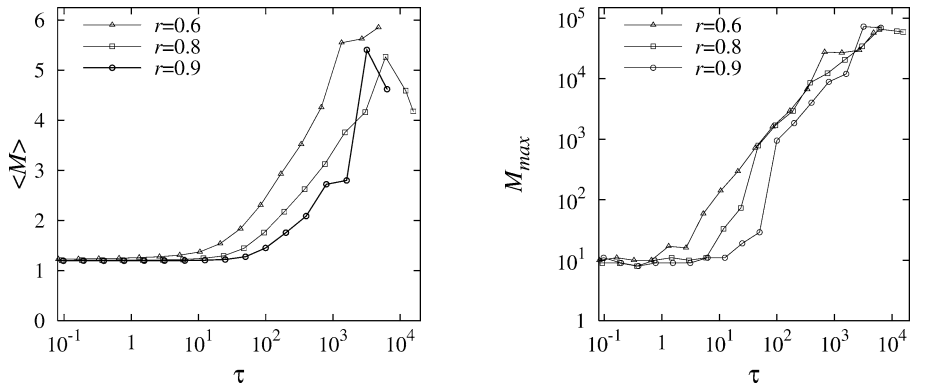

Figure 5. Mean cluster size (left) and maximum cluster size (right) as functions of time τ.

cluster growth startes earlier for stronger dissipation, but the largest cluster seems to grow more rapidly for weaker dissipation, however, at a later time.

3.4. Probability distribution of the collision rate

For a more quantitative analysis of the clustering instability, the probability distribution for particle collision frequencies is examined. $P(\mathcal{C})$ gives the probability to find a particle that carried out $\mathcal{C}$ collisions in the time interval Δt. For an elastic, homogenous system with independent events, the Poisson distribution

$$P_o(\mathcal{C}) = \frac{\exp(\chi\,\Delta t)(\chi\,\Delta t)^{\mathcal{C}}}{\mathcal{C}!}, \tag{4}$$

with mean collision rate $\chi = \int \mathcal{C} P(\mathcal{C})\,\mathrm{d}\mathcal{C}$ describes the probability that a particle had $\mathcal{C}$ collisions in the time-interval Δt. Since the statistics is better for large Δt, the distribution broadens with decreasing Δt.

In Fig. 6, the probability distribution of the collision rate, $p_\mathrm{n} = P(t_\mathrm{n}^{-1})\,\Delta t$, is plotted against the collision rate $t_\mathrm{n}^{-1} = \mathcal{C}/\Delta t$, for the times τ corresponding to the snapshots in Fig. 1. The shape of p_n resembles a Poisson distribution with decreasing mean-value χ for $\tau \leqslant 40$ (only data for $\tau = 15.7$ are shown here).

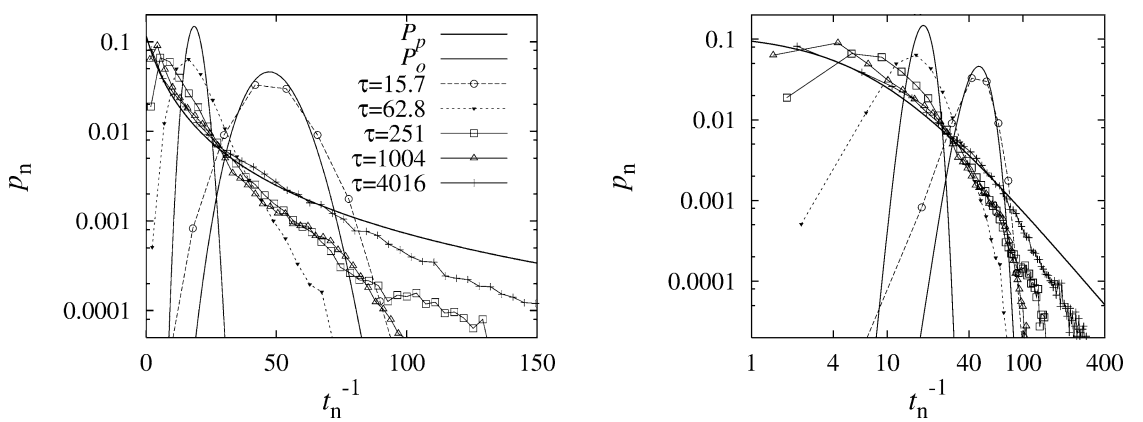

Figure 6. $P(\mathcal{C})$ for different τ-values from the simulation displayed in Fig. 1. The left panel contains a semi-log plot, whereas the right panel shows the same data in log-log-distribution. The solid curves P_o correspond to equation (4) and the symbols (connected by lines to guide the eye) are the simulation results.

However, due to the sampling of the data in the homogeneous cooling regime (where the collision rate changes with time), the agreement is not perfect. Using smaller time-intervals or elastic particles leads to reasonable agreement between p_{n} from simulations and the Poisson distribution p_o.

As soon as the clusters start to grow, the shape of the probability distribution changes. In Fig. 6, one observes a broadening of the initial Poisson distribution at $\tau = 62.8$, and for larger times, the convex shape has evolved to a slightly concave curve. The probability for large collision rates increases and can be approximated a power-law of the form

$$P_p(\mathcal{C}) = \frac{\chi}{(\chi + \mathcal{C})^2}, \tag{5}$$

in the final regime where the clusters are as large as the system. Even though the shape is well approximated by this curve, there is a cut-off at huge collision rates, possibly due to the finite size of the system.

Note that the shape of the distribution function is only weakly varying in the cluster-growth regime, and it is almost stationary in the final regime of huge clusters. At large times, particles that carry out many collisions coexist with those which carry out only a few.

4. Summary and conclusion

With a rather simple description of a granular material as an ensemble of inelastic spherical particles we have investigated the interesting effect of clustering in freely cooling systems. For short times the system is disordered and gas-like, whereas the structures at larger times are dense, crystalline clusters. The clusters grow until they reach the system size. Simulations at very long times were possible with the TC model which reduces dissipation when contacts become too frequent.

The statistics of the particle collision frequencies were examined: the probability distribution of the collision frequencies shows two types of behavior. In the homogeneous, random regime the distribution resembles a Poisson distribution, indicating that the collisions are uncorrelated events. As soon as cooperative effects like clustering occur, the probability distribution changes to a power-law shape. We proposed functional forms that approximate the distribution functions measured from simulations for both regimes.

The described cooperative phenomenon of cluster growth leaves a fingerprint, i.e. a power-law, in the global distribution function. An open issue is the theoretical verification and understanding of the shape of the probability distribution function and, as usual, the examination of three-dimensional systems with numerical methods, theory and possibly experiments.

Acknowledgements. We acknowledge the financial support of the Deutsche Forschungsgemeinschaft (DFG).

References

[1] H.J. Herrmann, J.-P. Hovi, S. Luding (Eds.), Physics of Dry Granular Media, NATO ASI Series E, Vol. 350, Kluwer, Dordrecht, 1998.
[2] T. Pöschel, S. Luding (Eds.), Granular Gases, Lecture Notes in Physics, Vol. 564, Springer, Berlin, 2001.
[3] P.A. Vermeer, S. Diebels, W. Ehlers, H.J. Herrmann, S. Luding, E. Ramm (Eds.), Continuous and Discontinuous Modelling of Cohesive Frictional Materials, Lecture Notes in Physics, Vol. 568, Springer, Berlin, 2001.
[4] Y. Kishino (Ed.), Powders and Grains 2001, Balkema, Rotterdam, 2001.
[5] I. Goldhirsch, G. Zanetti, Clustering instability in dissipative gases, Phys. Rev. Lett. 70 (11) (1993) 1619–1622.
[6] S. McNamara, W.R. Young, Dynamics of a freely evolving, two-dimensional granular medium, Phys. Rev. E 53 (5) (1996) 5089–5100.
[7] S. Luding, H.J. Herrmann, Cluster growth in freely cooling granular media, Chaos 9 (3) (1999) 673–681.
[8] R. Cafiero, S. Luding, H.J. Herrmann, Two-dimensional granular gas of inelastic spheres with multiplicative driving, Phys. Rev. Lett. 84 (2000) 6014–6017.
[9] S. Luding, Surface waves and pattern formation in vibrated granular media, in: Powders and Grains, Vol. 97, Balkema, Amsterdam, 1997, pp. 373–376.

[10] S. Luding, J. Duran, E. Clément, J. Rajchenbach, Simulations of dense granular flow: Dynamic arches and spin organization, J. Phys. I (France) 6 (1996) 823–836.
[11] B.D. Lubachevsky, How to simulate billards and similar systems, J. Comput. Phys. 94 (2) (1991) 255.
[12] S. Luding, Granular materials under vibration: Simulations of rotating spheres, Phys. Rev. E 52 (4) (1995) 4442.
[13] P.A. Cundall, O.D.L. Strack, A discrete numerical model for granular assemblies, Géotechnique 29 (1) (1979) 47–65.
[14] M.P. Allen, D.J. Tildesley, Computer Simulation of Liquids, Oxford University Press, Oxford, 1987.
[15] M. Lätzel, S. Luding, H.J. Herrmann, Macroscopic material properties from quasi-static, microscopic simulations of a two-dimensional shear-cell, Granular Matter 2 (3) (2000) 123–135, cond-mat/0003180.
[16] S. Luding, Collisions and contacts between two particles, in: H.J. Herrmann, J.-P. Hovi, S. Luding (Eds.), Physics of Dry Granular Media, NATO ASI Series E, Vol. 350, Kluwer, Dordrecht, 1998, p. 285.
[17] S. Luding, S. McNamara, How to handle the inelastic collapse of a dissipative hard-sphere gas with the TC model, Granular Matter 1 (3) (1998) 113–128, cond-mat/9810009.
[18] S. Luding, E. Clément, A. Blumen, J. Rajchenbach, J. Duran, Anomalous energy dissipation in molecular dynamics simulations of grains: The “detachment effect”, Phys. Rev. E 50 (1994) 4113.
[19] S. Luding, E. Clément, A. Blumen, J. Rajchenbach, J. Duran, Interaction laws and the detachment effect in granular media, in: Fractal Aspects of Materials, Symposium Proceedings, Vol. 367, Materials Research Society, Pittsburgh, Pennsylvania, 1995, pp. 495–500.
[20] P.K. Haff, Grain flow as a fluid-mechanical phenomenon, J. Fluid Mech. 134 (1983) 401–430.
[21] S. Luding, M. Huthmann, S. McNamara, A. Zippelius, Homogeneous cooling of rough dissipative particles: Theory and simulations, Phys. Rev. E 58 (1998) 3416–3425.